**Supplementary Information for**

**Endoscopic detection of cancer with lensless radioluminescence imaging and machine vision**

Silvan Türkcan[1], Dominik J Naczynski[1], Rosalie Nolley[2], Laura Sasportas[3,4], Donna M Peehl[2], Guillem Pratx[1,*]

[1]Medical Physics, Stanford University School of Medicine, Stanford, CA 94305, USA

[2]Department of Urology, Stanford University School of Medicine, Stanford, CA 94305, USA

[3]Department of Radiology, Stanford University School of Medicine, Stanford, CA 94305, USA

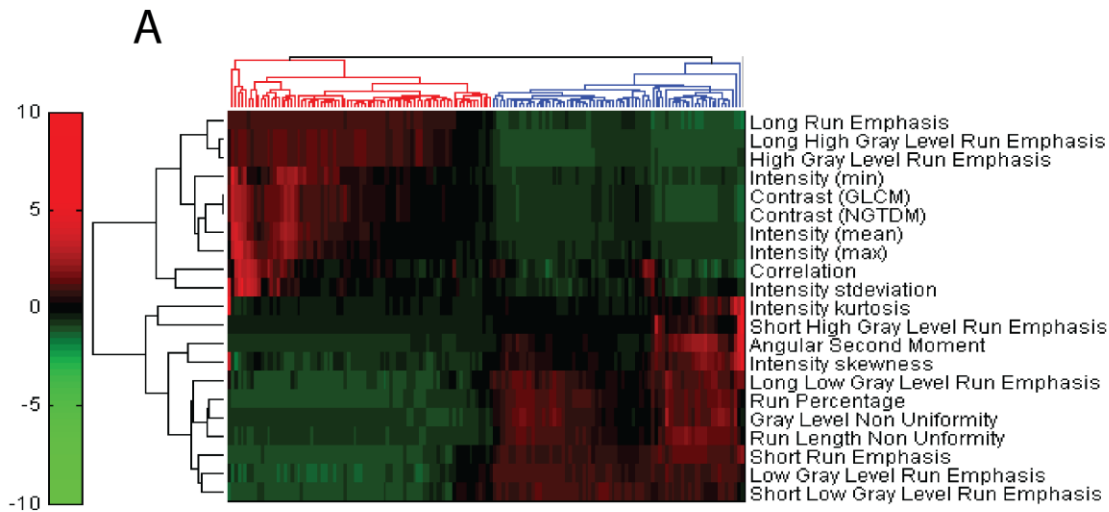[4]Department of Bioengineering, Stanford University, Stanford, CA 94305, USA

*Correspondence: pratx@stanford.edu

Figure S1

Table S2

Table S3

Table S4

# A



# B

Z-Score ([Value-Mean]/StdDev)

| | Cancer | Cancer | Cancer | Cancer | Cancer | Cancer | Normal | Normal | Normal | Normal | Normal | Normal |
|---|---|---|---|---|---|---|---|---|---|---|---|---|
| 'Long Run Emphasis' | 1.22 | 1.22 | 1.08 | 1.09 | 0.71 | -0.28 | -0.62 | -0.85 | -0.97 | -0.45 | -1.14 | -1.17 |
| 'Long High Gray Level Run Emphasis' | 1.32 | 1.35 | 1.11 | 1.11 | 0.70 | -0.56 | -0.86 | -0.96 | -0.98 | -0.67 | -1.00 | -1.01 |
| 'High Gray Level Run Emphasis' | 1.32 | 1.35 | 1.11 | 1.11 | 0.70 | -0.58 | -0.87 | -0.98 | -0.98 | -0.68 | -0.99 | -1.01 |
| 'Intensity (min)' | 4.38 | 2.23 | 1.11 | -0.05 | 0.32 | -0.39 | -0.80 | -0.70 | -0.85 | -0.47 | -0.69 | -0.81 |
| 'Contrast (GLCM)' | 3.22 | 1.85 | 1.03 | 0.58 | -0.14 | -0.40 | -0.39 | -0.83 | -0.81 | -0.35 | -1.06 | -0.91 |
| 'Contrast (NGTDM)' | 3.22 | 1.85 | 1.03 | 0.58 | -0.14 | -0.40 | -0.39 | -0.83 | -0.81 | -0.35 | -1.06 | -0.91 |
| 'Intensity (mean)' | 3.68 | 2.35 | 0.81 | 0.17 | -0.05 | -0.47 | -0.52 | -0.75 | -0.73 | -0.46 | -0.86 | -0.82 |
| 'Intensity (max)' | 3.08 | 1.74 | 0.37 | -0.05 | -0.03 | -0.49 | -0.23 | -0.72 | -0.65 | -0.67 | -0.84 | -0.72 |
| 'Correlation' | -0.28 | 1.84 | -0.56 | 0.02 | -0.38 | -0.78 | 0.86 | -0.70 | -0.20 | 0.57 | -0.99 | -0.45 |
| 'Intensity stdeviation' | 0.53 | 0.38 | -0.14 | -0.60 | -0.30 | -0.34 | 0.20 | -0.64 | -0.47 | -0.46 | -0.67 | -0.17 |
| 'Intensity kurtosis' | -0.51 | -0.71 | -0.54 | -0.53 | -0.50 | -0.66 | -0.09 | 0.13 | -0.18 | -0.65 | 0.67 | 1.36 |
| 'Short High Gray Level Run Emphasis' | -0.52 | -0.52 | -0.54 | -0.54 | -0.52 | -0.45 | -0.09 | -0.16 | 0.21 | -0.35 | 1.26 | 0.51 |
| 'Angular Second Moment' | -0.81 | -0.82 | -0.72 | -0.72 | -0.59 | -0.48 | -0.39 | 0.35 | 0.38 | -0.52 | 1.59 | 1.14 |
| 'Intensity skewness' | -0.98 | -0.91 | -1.17 | -0.65 | -1.03 | -0.78 | 0.08 | 0.54 | 0.37 | -0.34 | 1.20 | 1.48 |
| 'Long Low Gray Level Run Emphasis' | -1.23 | -1.01 | -0.99 | -1.17 | -1.10 | -0.24 | 1.07 | 0.88 | 0.62 | 0.02 | 1.26 | 1.22 |
| 'Run Percentage' | -1.02 | -1.02 | -0.99 | -0.99 | -0.92 | -0.28 | 0.49 | 1.08 | 1.01 | -0.12 | 1.15 | 1.51 |
| 'Gray Level Non Uniformity' | -0.85 | -0.85 | -0.90 | -0.90 | -0.97 | -0.57 | 0.54 | 1.14 | 0.79 | -0.37 | 1.01 | 1.68 |
| 'Run Length Non Uniformity' | -0.92 | -0.92 | -0.91 | -0.91 | -0.93 | -0.50 | 0.02 | 1.03 | 0.90 | -0.29 | 1.59 | 1.47 |
| 'Short Run Emphasis' | -1.11 | -1.11 | -1.12 | -1.12 | -0.70 | 0.21 | 0.48 | 0.89 | 0.93 | 0.33 | 1.30 | 1.14 |
| 'Low Gray Level Run Emphasis' | -1.33 | -1.22 | -1.10 | -1.18 | -0.82 | 0.39 | 1.07 | 1.08 | 0.82 | 0.55 | 0.92 | 1.12 |
| 'Short Low Gray Level Run Emphasis' | -1.18 | -1.18 | -1.20 | -1.20 | -0.51 | 0.82 | 0.81 | 1.27 | 0.91 | 0.80 | 0.83 | 0.91 |

**Figure S1: Clustering of ROIs based on the Z-Scores of the image features.** (a) Clustering result of the small ROIs in Fig. 6c based on the feature. Red shows higher than mean values calculated from the Z-score, while green represents below average values. (b) The Z-scores of some of the matrix elements in the clustergram in a.

|  | Cancer ROIs | False negatives | Normal ROIs | False positives |
|---|---|---|---|---|
| Sample 1 | 78 | 17 (22%) | 78 | 61 (22%) |
| Sample 2 | 52 | 12(23%) | 52 | 11 (21%) |
| Sample 3 | 62 | 16 (26%) | 62 | 16 (25%) |
| Sample 4 | 78 | 16 (21%) | 78 | 14 (18%) |
| Sample 5 | 44 | 10 (23%) | 44 | 9 (21%) |
| Mean |  | **23±2%** |  | **21±3%** |

**Table S4: Performance in tumor samples.** We measure the performance of the imaging system in 5 tumor samples.

|  | Mean C | Mean N | TNR |
|---|---|---|---|
| min | 31.84 | 12.08 | 2.64 |
| max | 43.32 | 25.26 | 1.71 |
| mean | 37.03 | 17.25 | 2.15 |
| stdeviation | 2.43 | 2.43 | 1.00 |
| skewness | 0.59 | 1.21 | 0.49 |
| kurtosis | 3.70 | 4.97 | 0.74 |
| Short Run Emphasis | 0.14 | 0.35 | 0.40 |
| Long Run Emphasis | 860.44 | 639.92 | 1.34 |
| Gray Level Non Uniformity | 18.24 | 44.59 | 0.41 |
| Run Length Non Unformity | 39.30 | 65.06 | 0.60 |
| Run Percentage | 0.10 | 0.22 | 0.46 |
| Low Gray Level Run Emphasis | 0.24 | 0.48 | 0.50 |
| High Gray Level Run Emphasis | 163.25 | 52.60 | 3.10 |
| Short Low Gray Level Run Emphasis | 0.11 | 0.23 | 0.50 |
| Short High Gray Level Run Emphasis | 0.49 | 2.14 | 0.23 |
| Long Low Gray Level Run Emphasis | 109.43 | 232.66 | 0.47 |
| Long High Gray Level Run Emphasis | 166807.29 | 51690.14 | 3.23 |
| Angular 2nd Moment | 0.06 | 0.22 | 0.29 |
| Contrast (GLCM) | 4.22 | 2.25 | 1.88 |
| Correlation | 0.26 | 0.27 | 0.96 |
| Contrast (NGTDM) | 4.22 | 2.25 | 1.88 |

| SUM: | 17.51 |
|---|---|

**Table S3: Tumor to normal ratio from machine vision.** We show the tumor to normal (TNR) for each of the image features. Summing up the features gives improves the TNR from the initially 2.1 to 17.51. This is an 8 fold increase.

| Sample | 1 | 2 | 3 | 4 | 5 | | Mean | STD |
|---|---|---|---|---|---|---|---|---|
| TNR simple | 2.1 | 3.5 | 2.2 | 4.6 | 1.9 | | 2.9 | 1.2 |
| TNR features | 17.51 | 20.45 | 17.73 | 59.20 | 14.12 | | 26 | 19 |
| Fold improvement | 8.3 | 5.8 | 8.2 | 12.7 | 7.6 | | 9 | 3 |

**Table S4: Fold improvement in TNR for all samples.** The average fold improvement in TNR from the image features is 9±3 for all samples.